

Fuzzy affinity hydration model

Wilson Ricardo Leal da Silva* and Vít Šmilauer

Czech Technical University in Prague, Faculty of Civil Engineering, Department of Mechanics, Thákurova 7, 166 29 Prague 6, Czech Republic

Abstract. Time-dependent hydration process of Portland cement presents a complex system with several uncertainties. A presented four-parametric affinity hydration model captures well the hydration kinetics when three parameters are treated as fuzzy numbers. The equations for the fuzzy affinity hydration model are derived using Zadeh's extension principle, which allows for simplifying calculations to obtain a fuzzy solution. The fuzzy model validates Portland cements with different mineral compositions, water-cement ratios ranging from 0.16 to 0.50, and curing temperatures varying from 10 to 30°C. Also, the fuzzy model is verified against CEMHYD3D and s-shape hydration model. In summary, validation and verification results show that the fuzzy model permits to predict vague conditions without lacking the credibility of results.

Keywords: affinity hydration model, cement hydration, extension principle, fuzzy numbers, modeling

1. Introduction

Hydration kinetics of Ordinary Portland Cement (OPC) is of paramount importance since it determines strength evolution, creep rate, permeability, or heat release during concrete hardening. The complexity of cement hydration occurs primarily due to an influence of four mineral clinker phases, impurities, and their interactions [33]. The degree of hydration (DoH), which is defined as the total weight fraction of reacted Portland cement, quantifies the hydration extent.

Several experimental methods, e.g. calorimetry, non-evaporable water content, SEM image analysis, chemical shrinkage, and X-ray diffraction analysis (QXDA), have been proposed and applied to determine the degree of hydration [29, 33]. A comprehensive list of experimental methods is summarized in [35].

Experimental investigations serve as basis for validating deterministic prediction models of cement hydration, which are extensively used due to their

practicality. Examples of well-known deterministic hydration models include the CEMHYD3D model based on cellular automata [3], the model based on the theory of reactive porous media [9], the general hydration model equation (s-shape model) introduced in [32], and the affinity hydration model [6]. For additional examples and comparisons of hydration models refer to [41]. Particular attention has been given to the affinity hydration model in recent applications [11, 21] due to its relatively low number of input parameters and robustness when simulating hydration kinetics of modern cements (i.e. blended cements), which contain at least one supplementary material, e.g. blast-furnace slag, and one chemical admixture [1].

The objective of this paper is extending microstructure-property link to a broad range of OPCs. This means relating model parameters (chemical composition, temperature, w/c ratio) of evolving microstructures to the evolution of hydration degrees. In the view of multiscale simulations, the hydration model evaluation in many integration points requires a time-efficient approach, penalizing time-consuming models such as CEMHYD3D. Concurrently, a hydration model needs to cover experimental data including the variability in microstructures, which stems from

*Corresponding author. Wilson Ricardo Leal da Silva, Czech Technical University in Prague, Faculty of Civil Engineering, Dept. of Mechanics, Thákurova 7, 166 29 Prague 6, Czech Republic. Tel.: +420 224 354 629; Fax: +420 224 310 775; E-mail: wilson.silva@fsv.cvut.cz.

cement production, experimental methods, and their errors. As a consequence of these requirements, a fuzzy version of the deterministic affinity hydration model is introduced.

Experimental data on the evolution of cement hydration are seldom available due to time, equipment, and budget constraints. Besides, engineers tend to bind to cement designations specified in technical standards rather than its true properties. These issues combined favor microstructure-property models against purely phenomenologically-based models.

This paper introduces fuzzy set theory to three parameters of the affinity hydration model. The parameters are linked to cement mineral composition and *Blaine* fineness while accounting for the variability of cement properties. In addition, a fuzzy version of the affinity hydration model is derived based on Zadeh's extension principle [46]. The presented model as well as its microstructure-link are validated for OPC pastes with water-cement ratio ranging from 0.16 to 0.50, curing temperatures ranging from 10 to 30°C, and five mineral compositions. Also, the fuzzy model is verified against CEMHYD3D [3] and s-shape hydration model [32].

2. Affinity hydration model

The affinity hydration model provides a framework for accommodating all stages of cement hydration under isothermal temperature at 25°C. The rate of hydration $\frac{dDoH}{dt}$ can be expressed by

$$\frac{dDoH}{dt} = \bar{A}_{25}(DoH), \quad (1)$$

where $\bar{A}_{25}(DoH)$ corresponds to the chemical affinity, which has a dimension of time^{-1} .

The affinity for isothermal temperature can be obtained experimentally; specifically, the isothermal calorimetry measures a heat flow $q(t)$, which gives the hydration heat $Q(t)$ after integration. Cervera et al. [6] proposed an analytical form of the normalized affinity, which was further refined by Gawin et al. [19]. In this work, a slightly modified formulation, proposed in [21], is taken into account

$$\bar{A}_{25}(DoH) = \beta_1 \left(\frac{\beta_2}{DoH_\infty} + DoH \right) \cdot (DoH_\infty - DoH) \cdot \exp\left(-\eta \frac{DoH}{DoH_\infty}\right), \quad (2)$$

Table 1
Parameters for the affinity hydration model ($DoH_\infty = 0.85$)

Cement	$\beta_1, [h^{-1}]$	$\beta_2, [-]$	$\eta, [-]$
CEM I 32.5R Mitani ⁽¹⁾	0.5846	1.4e-3	7.0
CEM I 42.5R Mokra ⁽¹⁾	1.2667	8.0e-6	7.4
CEM I 42.5R Prachovice ⁽²⁾	0.9744	7.0e-4	6.7
CEM I 52.5R Princigallo ⁽²⁾	1.3641	6.0e-5	5.8
CEM II/A-S 42.5 Mokra ⁽¹⁾	0.9744	7.0e-4	6.7
CEM II/B-S 32.5R Mokra ⁽¹⁾	0.9744	7.0e-4	6.7
CEM III/B 32.5 Mokra ⁽¹⁾	0.5846	5.0e-3	8.0

⁽¹⁾isothermal calorimetry and ⁽²⁾CEMHYD3D model.

where β_1 and β_2 are parameters to be adjusted, η presents the micro-diffusion of free water through formed hydrates, and DoH_∞ is the ultimate degree of hydration. These parameters express isothermal hydration at 25°C. When hydration proceeds under varying temperature T , \bar{A}_{25} can be scaled via Arrhenius equation

$$\bar{A}_T = \bar{A}_{25} \cdot \exp\left[\frac{E_a}{R} \cdot \left(\frac{1}{298.15} - \frac{1}{T}\right)\right], \quad (3)$$

where R [$\text{Jmol}^{-1}\text{K}^{-1}$] is the universal gas constant and E_a [Jmol^{-1}] is the activation energy. The evolution of DoH is obtained through numerical integration since there is no analytical exact solution.

The affinity hydration model performs well on OPC and blended cements. The validation of the affinity hydration model against isothermal calorimetry data or CEMHYD3D [3] simulation is depicted in Fig. 1, capturing water/binder ratios in the range from 0.40 to 0.50. The parameters considered in the simulations are listed in Table 1. The cement designation used in Table 1 is in accordance with the European standard EN 197-1 [17]. In all cases, DoH_∞ was set at 0.85 and the results were scaled to isothermal temperature 25°C by recalculating them with $E_a = 38.3 \text{ kJmol}^{-1}$. Further applications of the affinity hydration model are available elsewhere [11, 21, 39]. Also, an open-source cross-platform desktop application, namely CEMHapp©, that uses the affinity hydration model to predict the degree of hydration may be freely downloaded and used [14].

The results from the affinity model, CEMHYD3D, the s-shape hydration model described in Equation (4) [32], and isothermal calorimetry for CEM I 42.5R Mokra are compared in Fig. 2. The experimental measurements and CEMHYD3D model's parameters were collected from [10, 21]; whereas the parameters of the s-shape curve were calibrated to obtain the most reasonable predictions at early and later stages. In all cases, DoH_∞ was set at 0.85.

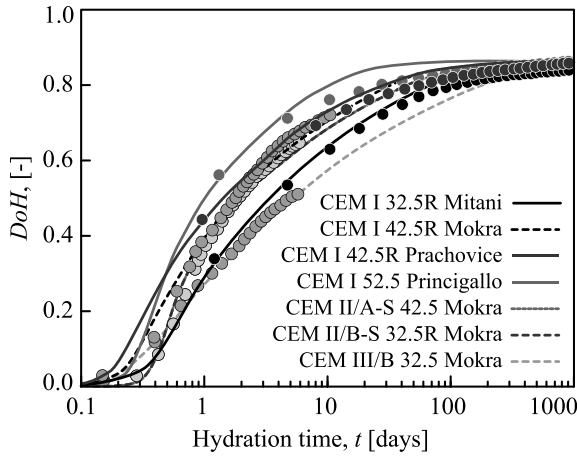


Fig. 1. Validation of affinity hydration model on various cement types, water/binder ratios from 0.40 to 0.50.

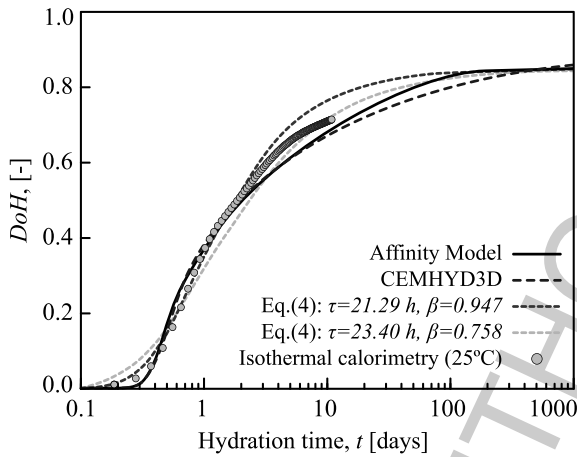


Fig. 2. Comparison of the affinity hydration model, CEMHYD3D [3], the s-shape model (Equation (4)) [32], and isothermal measurements of CEM I 42.5R Mokra, at $w/c = 0.50$ [10, 21].

$$DoH(t) = DoH_{\infty} \cdot \exp\left(-\left[\frac{\tau}{t}\right]^{\beta}\right), \quad (4)$$

where τ and β are the hydration time [h] and shape parameter [-], respectively. For more details on the hydration model from Equation (4) refer to [32].

Figures 1 and 2 prove successful the deterministic version of the affinity hydration model against different modeling techniques and experimental results. The advantage of the affinity hydration model relies on the fact that only few parameters have to be calibrated to predict cement hydration kinetics. Despite Equation (4) having less parameters and performing reasonably well on non-blended cements [32], prediction mismatches

are likely observed at either early ($t = 1$ to 3 days) or later stages ($t > 14$ days) when simulating the kinetics of blended cements. Notice that, at present, blended cements represent the greatest share of commercialized cement and tend to contain less and less clinker [1]. Furthermore, proper DoH predictions at early and later stages are important when simulating concrete temperature and strength development.

The adequate performance of the affinity hydration model does not change the fact that its parameters (β_1 , β_2 , η , and DoH_{∞}) have to be determined based on expertise and/or experimental measurements followed by curve fitting methods, e.g. least-square method (LSM). To overcome the phenomenological characteristic of the affinity model, a microstructure-property link should be established, i.e. the model's parameters should be linked to cement properties.

Notice, however, that the production of cement is prone to variability, such that even cement batches from a common plant present slightly different compositions, within the range of values specified in technical standards, e.g. [2, 17]. For example, the clinker composition of Portland-slag cement (CEM II/A-S) must be within 80 to 94% [17]. Therefore, the link between affinity model's parameters and cement properties also carries a certain degree of vagueness despite its effectiveness.

Once this link is established, the input parameters of the affinity hydration model β_1 , β_2 , η , and DoH_{∞} become inherently uncertain and their representation by fuzzy numbers is therefore reasonable. Consequently, the final output as DoH also becomes a fuzzy number. The fuzziness, i.e. uncertainty or vagueness, in the predicted degree of hydration is likely more pronounced when a person without proper knowledge on cement hydration kinetics determines the model's parameters or when cement properties remain unknown.

Prior to presenting the fuzzy version of the affinity hydration model as well as its microstructure-link and application, a brief review on fuzzy sets and fuzzy numbers is introduced.

3. Fuzzy sets and fuzzy numbers

In 1965, Lotfi A. Zadeh developed the foundation of fuzzy set theory based on the concept of vagueness, which was first envisioned by Max Black in 1937 [24, 42, 46]. According to Zadeh [46], fuzzy sets are sets with boundaries that are not precise, i.e. there is a smooth transition from membership to non-membership, allowing for dealing with measurement

uncertainties and vagueness without compromising the reliability of the solution. Fuzzy set theory was applied in many disciplines to resolve vagueness and uncertainties, e.g. [12, 13, 28].

On fuzzy set theory, the degree of membership $\mu_{\tilde{B}}(x)$ of an element x in a fuzzy set \tilde{B} consists of an unit interval $[0,1]$. Thus, the classical set theory is verified when $\mu_{\tilde{B}}(x) = 1$ or $\mu_{\tilde{B}}(x) = 0$. Besides, values of $\mu_{\tilde{B}}(x)$ within $[0,1]$ are also accepted, allowing to describe any element x that partially belongs to \tilde{B} . Hence, fuzzy sets are considered as a generalization of classical sets. A fuzzy set \tilde{B} defined on the universe of discourse X can be formally declared as

$$\tilde{B} = \left\{ (x, \mu_{\tilde{B}}(x)) \mid x \in X \right\}, \quad (5)$$

If a fuzzy set is convex, normalized, and its membership function is defined on \mathbb{R}^1 and piecewise continuous, then this set is called a fuzzy number [25]. A fuzzy number is a fuzzy set with membership function that is upper-semicontinuous and normalized [18, 34]. Generally, a fuzzy number is defined as a real number whose boundary is fuzzy [25].

The membership function of a fuzzy set, or a fuzzy number, can assume several shapes, which will depend on the context of a particular application. Basically, the shape of a fuzzy set can be purely designed depending on the developer's expertise. According to Klir and Yuan [24], many applications are not overly sensitive to variations in the membership functions' shape. Thus, it is convenient to use simple shapes such as triangular shape; specifically, the membership function of a triangular fuzzy number \tilde{F} is declared as

$$\mu_{\tilde{F}}(x) = \begin{cases} 0 & , x < x_1 \vee x > x_3, \\ \frac{x - x_1}{x_2 - x_1} & , x_1 \leq x \leq x_2, \\ \frac{x_3 - x}{x_3 - x_2} & , x_2 < x \leq x_3. \end{cases} \quad (6)$$

where x_1 , x_2 , and x_3 are the boundaries of the fuzzy number, see Fig. 3. Alternatively, a triangular fuzzy number \tilde{F} can be described as $\tilde{F}(x_1, x_2, x_3; h)$, where h corresponds to the height of the fuzzy set.

Given a fuzzy set \tilde{B} defined on X and any number α within the unit interval $[0,1]$, the α -cut of \tilde{B} reads

$$\tilde{B}_\alpha = \left\{ x \mid \mu_{\tilde{B}}(x) \geq \alpha, x \in X \right\}. \quad (7)$$

The α -cut corresponds to a crisp interval (set) determined from the fuzzy set according to a selected membership function value, i.e. $\mu_{\tilde{B}}(x) = \alpha$. Basically,

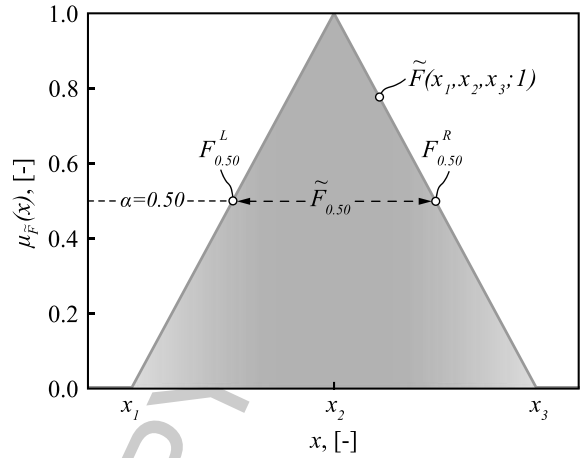


Fig. 3. Triangular fuzzy number $\tilde{F}(x_1, x_2, x_3; h)$, with $h = 1$.

any fuzzy set can be derived from a significant number of α -cut sets. The α -cut (\tilde{F}_α) of a triangular fuzzy number $\tilde{F}(x_1, x_2, x_3; 1)$ can be declared as

$$\tilde{F}_\alpha = [F_\alpha^L, F_\alpha^R], \quad (8)$$

where F_α^L and F_α^R are the left and right boundaries of the α -cut, respectively. F_α^L and F_α^R are computed by

$$F_\alpha^L = x_1 + (x_2 - x_1) \cdot \alpha \quad (9)$$

and

$$F_\alpha^R = x_3 - (x_3 - x_2) \cdot \alpha, \quad (10)$$

respectively. The α -cut $\tilde{F}_{0.50}$ as well as its boundaries ($F_{0.50}^L$ and $F_{0.50}^R$) are depicted in Fig. 3. As further discussed in Section 4, the combination of the α -cut representation and Zadeh's extension principle shown in Equations (8) and (19), respectively, helps simplifying calculations of the output from fuzzy functions.

Finally, the measure of fuzziness of a fuzzy set is introduced. A measure of fuzziness estimates the ambiguity present in a fuzzy set [44]. Although several methods have been introduced, e.g. [7, 8, 22, 43, 47], the measure of fuzziness based on Hamming distance, which is defined by the sum of absolute values of difference, is commonly used because it is simple and intuitively easy to comprehend [24]. Considering a triangular fuzzy number $\tilde{F}(x_1, x_2, x_3; 1)$, the corresponding measure of fuzziness $m(\tilde{F})$ is computed by

$$m(\tilde{F}) = x_3 - x_1 - \int_{x_1}^{x_3} |2\mu_{\tilde{F}}(x) - 1| dx, \quad (11)$$

and the degree of fuzziness $\gamma(\tilde{F})$ is given by a percentage of the central value, i.e.

$$\gamma(\tilde{F}) = \frac{m(\tilde{F})}{x_2}. \quad (12)$$

4. Fuzzy affinity hydration model

4.1. Vagueness in estimating parameters

The fuzziness of the input parameters β_1 , β_2 , η , and DoH_∞ will influence the fuzziness of the output DoH . In order to simplify calculations without compromising the reliability of results, it is important to investigate which of these parameters are uncertain.

The parameters β_1 , β_2 , and η can be estimated based on cement *Blaine* fineness and mineral composition, which have considerable influence on hydration kinetics [27, 37]. For example, ranges of *Blaine* fineness and mineral composition of two type I Portland cement are summarized in Table 2, these values were collected from [30]. The data prove that nominally similar cements differ in fineness and mineral composition with an impact on hydration kinetics.

For the above-mentioned reasons, β_1 , β_2 , and η are assumed as fuzzy numbers. The boundaries of $\tilde{\beta}_1$, $\tilde{\beta}_2$, and $\tilde{\eta}$, which are assumed to be triangular fuzzy numbers, must be determined by an expert based on an investigation of cement composition variability and/or experimental measurements.

The intermediary values of $\tilde{\beta}_1$, $\tilde{\beta}_2$, and $\tilde{\eta}$ shown in Table 2 were computed from the average mineral compositions, based on [27] for atmospheric pressure

$$\beta_1 = 0.738 \cdot C_3S^{-0.206} \cdot C_2S^{-0.128} \cdot C_3A^{0.161}, \quad (13)$$

$$\beta_2 = \frac{(-0.0767 \cdot C_4AF + 0.0184) \cdot B_f}{\beta_1 \cdot 350}, \quad (14)$$

$$\eta = 10.95C_3S + 11.25C_2S - 4.10C_3A - 0.892 \quad (15)$$

where B_f is the *Blaine* fineness of cement in m^2/kg and C_3S , C_2S , C_3A , and C_4AF are the mass percentages of each mineral. The degree of fuzziness $\gamma(\beta_1)$, $\gamma(\beta_2)$, and $\gamma(\tilde{\eta})$ come from Equation (11). Equations (13)–(15) were converted from Lin and Meyer [27] since the model proceeds at 25°C instead of 20°C. For such particular case, a multiplication factor of 1.32 for $E_a = 40.0 \text{ kJ mol}^{-1}$ was used, according to Equation (3).

Table 2
Portland cement properties obtained from [30] and estimated $\tilde{\beta}_1$, $\tilde{\beta}_2$, and $\tilde{\eta}$

	CEM I 42.5 R	CEM I 52.5 R
C_3S , [%]	51.0 – 67.5	54.5 – 67.5
C_2S , [%]	7.0 – 22.0	7.0 – 19.2
C_3A , [%]	6.0 – 9.0	6.0 – 14.1
C_4AF , [%]	10.0 – 10.0	4.4 – 10.0
<i>Blaine</i> , [m^2/kg]	335 – 450	440 – 500
$\tilde{\beta}_1$, [h^{-1}]	(0.69, 0.73, 0.80; 1)	(0.75, 0.76, 0.78; 1)
$\tilde{\beta}_2$, [$-$] $\times 10^{-2}$	(1.31, 1.67, 2.04; 1)	(2.04, 2.26, 2.41; 1)
$\tilde{\eta}$, [$-$]	(5.2, 6.9, 8.6; 1)	(5.6, 6.7, 8.1; 1)
$\gamma(\beta_1)$, [%]	7.6	1.8
$\gamma(\beta_2)$, [%]	21.7	8.0
$\gamma(\tilde{\eta})$, [%]	24.6	18.7

Regarding the ultimate degree of hydration (DoH_∞), the results indicate that DoH_∞ is related only to the water-cement ratio (w/c) [31]. The theoretical value of DoH_∞ is always limited to

$$\frac{w/c}{0.40} \leq 1.0 \quad (\text{sealed condition}) \quad (16)$$

or

$$\frac{w/c}{0.36} \leq 1.0 \quad (\text{saturated condition}) \quad (17)$$

due to unavailable capillary space for accommodating hydration products [20]. Recent publications [21, 27], on the other hand, show that DoH_∞ also depends on the cement *Blaine* fineness. For simplicity, DoH_∞ is assumed as a crisp number (fixed parameter) within the range of 0.80 to 1.00 and limited to the theoretical values mentioned above.

4.2. Proposed fuzzy affinity hydration model

Assuming that the vagueness stems from estimating β_1 , β_2 , and η , and that DoH_∞ is a crisp value, the fuzzy rate of hydration $\frac{d\widetilde{DoH}}{dt}$ can be written as

$$\frac{d\widetilde{DoH}}{dt} = \tilde{\beta}_1 \left(\frac{\tilde{\beta}_2}{DoH_\infty} + \widetilde{DoH} \right) \cdot (DoH_\infty - \widetilde{DoH}) \cdot \exp\left(-\tilde{\eta} \frac{\widetilde{DoH}}{DoH_\infty}\right). \quad (18)$$

Several methods for solving fuzzy differential equations are discussed [5]. In this work, the solution of Equation (18) will be based on Zadeh's extension principle [46], which states that the image of a fuzzy set \tilde{A} under a crisp-mapping function f can be expressed as a fuzzy set \tilde{B} . This principle can be seen as the extension

of crisp functions to act on fuzzy sets. In particular, considering that $f : X \rightarrow Y$ and that \tilde{A} is a given fuzzy set defined on X , then the fuzzy set \tilde{B} defined on Y can be computed by

$$\mu_{\tilde{B}}(y) = \sup_{x=f^{-1}(y)} \mu_{\tilde{A}}(x), \quad \forall y \in Y, \quad (19)$$

where f^{-1} is the complete preimage (or inverse image) of f . The identity shown in Equation (19) corresponds to Zadeh's extension principle. The "sup" operator in Equation (19) is necessary to avoid the ambiguity of results that occurs when f is a many-to-one function, i.e. $f(x_1) = f(x_2) = y$, but $x_1 \neq x_2$ and $\mu_{\tilde{A}}(x_1) \neq \mu_{\tilde{A}}(x_2)$, for x_1 and $x_2 \in X$.

If $f : X \rightarrow Y$ is a continuous function, \tilde{A} is a fuzzy set defined on X , such that its membership function is upper-semicontinuous and \tilde{A}_α is compact $\forall \alpha \in (0, 1)$, and \tilde{B} is a fuzzy set defined on Y , such that $\tilde{B} = F(\tilde{A})$, then the relation $F(\tilde{A})_\alpha = f(\tilde{A}_\alpha)$ holds. Hence, the α -cut of \tilde{B} is coincident with the image of the \tilde{A}_α obtained by f , i.e. $\tilde{B}_\alpha = f(\tilde{A}_\alpha)$.

The application of Zadeh's extension principle allows for using fuzzy numbers in crisp functions [23]. To simplify calculations, the α -cut of the fuzzy input parameters can be used to determine the α -cut of the fuzzy output; specifically, the α -cut \widetilde{DoH}_α for a given time t reads

$$\widetilde{DoH}_\alpha = \begin{cases} DoH_\alpha^L(t, \tilde{\beta}_1, \tilde{\beta}_2, \tilde{\eta}, DoH_\infty, \alpha) = \\ = \min\{DoH(t, \beta_1, \beta_2, \eta, DoH_\infty, \alpha) \mid \\ \mid \beta_1 \in \tilde{\beta}_{1\alpha}, \beta_2 \in \tilde{\beta}_{2\alpha}, \eta \in \tilde{\eta}_\alpha\}, \\ DoH_\alpha^R(t, \tilde{\beta}_1, \tilde{\beta}_2, \tilde{\eta}, DoH_\infty, \alpha) = \\ = \max\{DoH(t, \beta_1, \beta_2, \eta, DoH_\infty, \alpha) \mid \\ \mid \beta_1 \in \tilde{\beta}_{1\alpha}, \beta_2 \in \tilde{\beta}_{2\alpha}, \eta \in \tilde{\eta}_\alpha\}, \end{cases} \quad (20)$$

In case the monotonicity of the output function does not hold, an optimization process is required to determine the output extremes of \widetilde{DoH}_α for a given α -cut. Refer to [4, 36] for examples of application.

However, because DoH corresponds to a monotonic function in the space of the input variables, see Equation (2), the extreme values of \widetilde{DoH}_α , i.e. $[DoH_\alpha^L, DoH_\alpha^R]$ can be calculated based on the extreme values of the parameters' intervals. This approach further simplifies calculations when combined with Zadeh's extension principle since the need for optimization to compute the fuzzy output is excluded.

This way, based on Equation (20) and considering the fuzzy input parameters $\tilde{\beta}_1$, $\tilde{\beta}_2$, and $\tilde{\eta}$ as triangular fuzzy numbers, see Equation (8), \widetilde{DoH}_α for a given time t is computed by

$$\widetilde{DoH}_\alpha = \begin{cases} DoH_\alpha^L(t, \tilde{\beta}_1, \tilde{\beta}_2, \tilde{\eta}, DoH_\infty, \alpha) = \\ = DoH(t, \beta_1^L, \beta_2^L, \eta^R, DoH_\infty, \alpha), \\ DoH_\alpha^R(t, \tilde{\beta}_1, \tilde{\beta}_2, \tilde{\eta}, DoH_\infty, \alpha) = \\ = DoH(t, \beta_1^R, \beta_2^R, \eta^L, DoH_\infty, \alpha). \end{cases} \quad (21)$$

Subsequently, \widetilde{DoH}_α is obtained by substituting Equation (21) in Equation (18), i.e.

$$\frac{dDoH_\alpha^L}{dt} = \beta_1^L \left(\frac{\beta_2^L}{DoH_\infty} + DoH_\alpha^L \right) \cdot (DoH_\infty - DoH_\alpha^L) \cdot \exp\left(-\eta^R \frac{DoH_\alpha^L}{DoH_\infty}\right) \quad (22)$$

and

$$\frac{dDoH_\alpha^R}{dt} = \beta_1^R \left(\frac{\beta_2^R}{DoH_\infty} + DoH_\alpha^R \right) \cdot (DoH_\infty - DoH_\alpha^R) \cdot \exp\left(-\eta^L \frac{DoH_\alpha^R}{DoH_\infty}\right), \quad (23)$$

and integrating Equations (22) and (23) over time. Finally, \widetilde{DoH} is derived from a significant number of α -cut for a given time t and its fuzziness is computed by Equation (11).

An example of the output from the fuzzy affinity hydration is depicted in Fig. 4(a). The fuzzy output \widetilde{DoH} was obtained based on the parameters from Table 2 ($DoH_\infty = 0.85$) and Equations (22) and (23), which were integrated over time. The fuzzy degree of hydration \widetilde{DoH} for $t = 1, 7, \text{ and } 28$ days is shown in Fig. 4(b).

The complexity analysis of the proposed hydration model is determined from an asymptotic sense considering the worst-case scenario; specifically, the O -notation [45] is used as a reference since it indicates the upper bound of the model's asymptotic behavior. The basic version of the affinity model, see Equation (2), presents a linear behavior, i.e. $O(n)$, as a result of the time integration that is applied to compute DoH .

The fuzzy model, conversely, features an $O(n^4)$ complexity at a particular time t . Such complexity yields

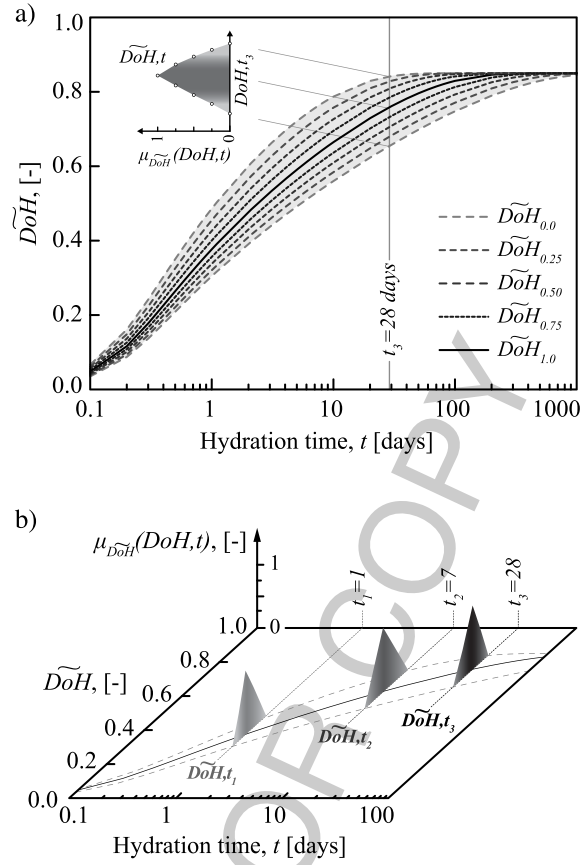


Fig. 4. a) Fuzzy hydration for CEM I 42.5 R and b) the corresponding \widetilde{DoH} for $t = 1, 7$, and 28 days.

from the iteration process over α and the fuzzy parameters $\widetilde{\beta}_1$, $\widetilde{\beta}_2$, and $\widetilde{\eta}$. After applying Zadeh's extension principle, the complexity of fuzzy model is reduced to $O(n)$ because the iteration over $\widetilde{\beta}_1$, $\widetilde{\beta}_2$, and $\widetilde{\eta}$ is excluded. Taking into account the time integration that is used to compute DoH , the complexity of the fuzzy model (Equations (18)–(20)) is then $O(n^5)$, whereas the complexity of the fuzzy model with extension principle (Equations (22)–(23)) is $O(n^2)$.

5. Application of the fuzzy affinity hydration model

The fuzzy affinity hydration model described in Section 4 was applied to predict OPC hydration. The obtained results were validated against experimental results available in the literature, specifically [15, 16, 26, 27, 38], and verified against CEMHYD3D [3] and the s-shape model [32] (Equation (4)). The following nomenclature was adopted:

- A:** cement pastes with the same type of cement and w/c but different curing temperatures (T_c) [15, 16].
- B:** cement pastes with the same type of cement and T_c but different w/c [27, 38].
- C:** cement pastes with the same w/c and T_c but different cement compound composition [26, 27].

The cement mineral composition, *Blaine* fineness, curing temperature and w/c of the pastes are summarized in Table 3.

The parameters adopted for the fuzzy affinity model are listed in Table 4. Their values were estimated based on the discussion presented in Section 4.1 and Table 2. The degree of fuzziness $\gamma(\widetilde{\beta}_1)$, $\gamma(\widetilde{\beta}_2)$, and $\gamma(\widetilde{\eta})$ were set at 5%, 15%, and 20%, respectively. The E_a values shown in Table 4 were collected from [15, 16, 26, 27, 38].

With regard to the verification of the fuzzy affinity model against other prediction models, the parameters from the s-shape model are listed in Table 5. Because

Table 3
Cement composition and experimental conditions [15, 16, 26, 27, 38]

Series	T_c	w/c	Mineral composition, [%]				Blaine [m ² /kg]
	[°C]		[-]	C ₃ S	C ₂ S	C ₃ A	
A1	10 ⁽⁴⁾	0.50	71.6	10.9	3.7	10.7	376
A2	20 ⁽⁴⁾	0.50	71.6	10.9	3.7	10.7	376
A3	30 ⁽⁴⁾	0.50	71.6	10.9	3.7	10.7	376
B1	25	0.16	41.4	34.0	9.8	7.5	368
B2	25	0.35	41.4	34.0	9.8	7.5	368
B3	25	0.50	41.4	34.0	9.8	7.5	368
C1	24	0.50	51.4	22.6	11.1	7.9	372
C2	24	0.50	41.6	34.4	5.4	13.2	314
C3	24	0.50	60.0	13.5	8.9	8.1	564

⁽⁴⁾ $T_c = 20^\circ\text{C}$ in the first 24 h [16].

the s-shape model does not present a microstructure-property relation, the parameters β and τ had to be determined by LSM in order to fit the predicted to the available measured data. The DoH_∞ , on the other hand, is equal to the ones used in the fuzzy model, see Table 4.

The cement properties shown in Table 3 were used as input for CEMHYD3D. Moreover, the random seed, representative volume element (RVE), induction time (t_0), and cycle-time mapping ($\beta_{CEMHYD3D}$) were set at 100, 50 μm , 0.0 h, and 3×10^{-4} , respectively, in all simulations. These values agree with the ones implemented in [39]. The CEMHYD3D calculations were performed using the CemPy application [40], which was developed at the Czech Technical University in Prague and may be freely downloaded and used.

5.1. Results and discussion

Figure 5 verifies the fuzzy affinity hydration model against the s-shape model Equation (4) [32] and CEMHYD3D [3]. Notice that, because the output from CEMHYD3D and Equation (4) are crisp values, only the most possible output from the fuzzy model, i.e. $\widetilde{DoH}_{1,00}$ is indicated in Fig. 5. The scatter plot of results and corresponding coefficient of determination (r^2) are displayed in Fig. 7.

When analyzing the results from the evaluated models (Figures 5 and 7), it is important to bear in mind that the s-shape model [32] enables proper DoH predictions because the model's parameters (Table 5) were fit based on experimental data. The same is not true for CEMHYD3D and the fuzzy affinity model, which feature a microstructure-link. In spite of that, all models present a similar trend with regard to DoH for the evaluated OPC.

Table 4
Estimated parameters of the fuzzy affinity hydration model

Series	Estimated parameters		
A	A1 to A3 [15, 16]	$\widetilde{\beta}_1$, [h ⁻¹]	(0.5866, 0.6175, 0.6484; 1)
		$\widetilde{\beta}_2$, [-]	(0.0151, 0.0177, 0.0204; 1)
		$\widetilde{\eta}$, [-]	(6.4153, 8.0192, 9.6230; 1)
		DoH_∞ , [-]	0.95
		E_a , [J/mol]	44166
		B	B1 to B3 [27, 38]
$\widetilde{\beta}_2$, [-]	(0.0162, 0.0190, 0.0219; 1)		
$\widetilde{\eta}$, [-]	(5.6499, 7.0624, 8.4749; 1)		
DoH_∞ , [-]	0.44, 0.80, and 0.90 ⁽⁵⁾		
E_a , [J/mol]	43000		
C	C1 [26, 27]		
		$\widetilde{\beta}_2$, [-]	(0.0155, 0.0182, 0.0210; 1)
		$\widetilde{\eta}$, [-]	(5.4569, 6.8211, 8.1854; 1)
		DoH_∞ , [-]	0.90
		E_a , [J/mol]	45721
		C2 [26, 27]	$\widetilde{\beta}_1$, [h ⁻¹]
	$\widetilde{\beta}_2$, [-]		(0.0100, 0.0117, 0.0135; 1)
	$\widetilde{\eta}$, [-]		(5.8478, 7.3097, 8.7717; 1)
	DoH_∞ , [-]		0.90
	E_a , [J/mol]		41778
	C3 [26, 27]		$\widetilde{\beta}_1$, [h ⁻¹]
		$\widetilde{\beta}_2$, [-]	(0.0233, 0.0274, 0.0315; 1)
$\widetilde{\eta}$, [-]		(5.4631, 6.8289, 8.1946; 1)	
DoH_∞ , [-]		1.00	
E_a , [J/mol]		49995	

⁽⁵⁾B1, B2, and B3, respectively.

Table 5
 DoH_∞ and parameters determined by LSM for Equation (4) [32]

Series	β , [-]	τ , [h]	DoH_∞ , [-]
A1	0.400	33.68	0.95
A2	0.428	23.86	0.95
A3	0.414	16.12	0.95
B1	0.432	10.59	0.44
B2	0.435	14.05	0.80
B3	0.470	18.13	0.90
C1	0.479	17.20	0.90
C1	0.451	23.06	0.90
C3	0.514	10.64	1.00

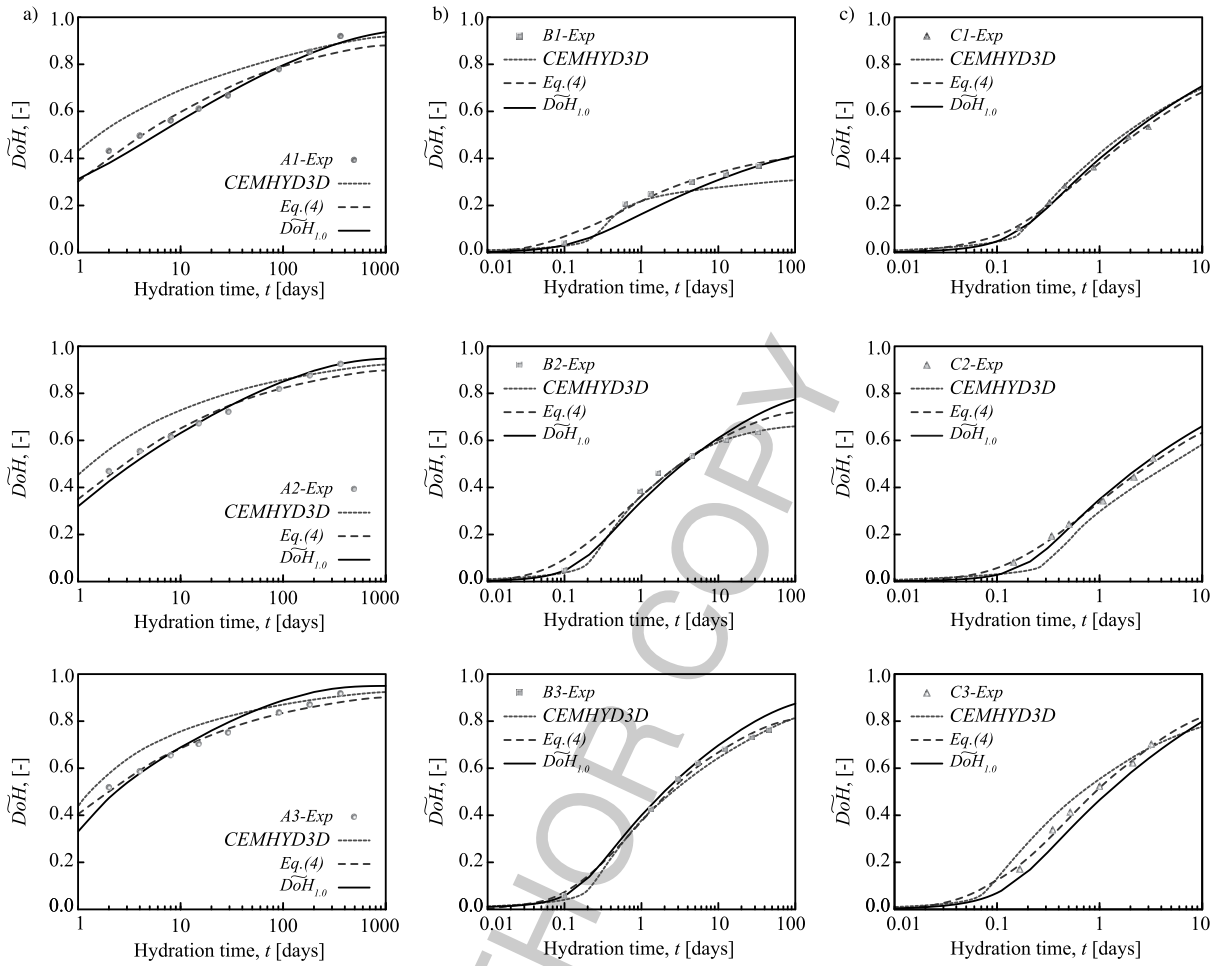


Fig. 5. Verification of fuzzy hydration against the hydration model from [32] and CEMHYD3D [3]: a) A1 to A3, b) B1 to B3, and c) C1 to C3.

The advantage of the fuzzy affinity hydration model over the s-shape model stems from its microstructure-property characteristic discussed throughout the paper. When compared to CEMHYD3D, conversely, different measures must be used since both the models have a microstructure-property link. Considering that DoH predictions are generally applied for estimating concrete's thermal behavior and strength development, to mention a few, and that such estimations depend on the evaluation of hydration model in several integration points, it is evident that a time-efficient approach is desired. Thus, the proposed model is advantageous over CEMHYD3D with regards to the model's complexity; specifically, CEMHYD3D model has a cubic-time behavior, i.e. $O(n^3)$, while the fuzzy model has a quadratic-time behavior $O(n^2)$.

Regarding the validation of the proposed model, Fig. 6 validates the simulation results for series

A, **B**, and **C**. Experimental data in Fig. 6(a) agree well with the fuzzy affinity hydration model for curing temperatures between 10 and 30°C in series **A**. In addition, it is clear that the degree of fuzziness considered for the input parameters, i.e. $\gamma(\beta_1)$, $\gamma(\beta_2)$, and $\gamma(\tilde{\eta})$, was properly estimated since all experimental points belong to the interval $[DoH_{0,0}^L, DoH_{0,0}^R]$ at any given time. In fact, the estimated degree of fuzziness could be further reduced once that the experimental data stay within the interval $[DoH_{0,25}^L, DoH_{0,25}^R]$.

Series **B** from Fig. 6(b) validates well pastes with w/c between 0.35 and 0.50 but not 0.16. For data sets B2, B3, the values assigned to $\gamma(\beta_1)$, $\gamma(\beta_2)$, and $\gamma(\tilde{\eta})$ could be reduced since the experimental results tend to stay within the interval $[DoH_{0,25}^L, DoH_{0,25}^R]$. For B1, simulation results indicate that the fuzziness of the parameters should be increased in order

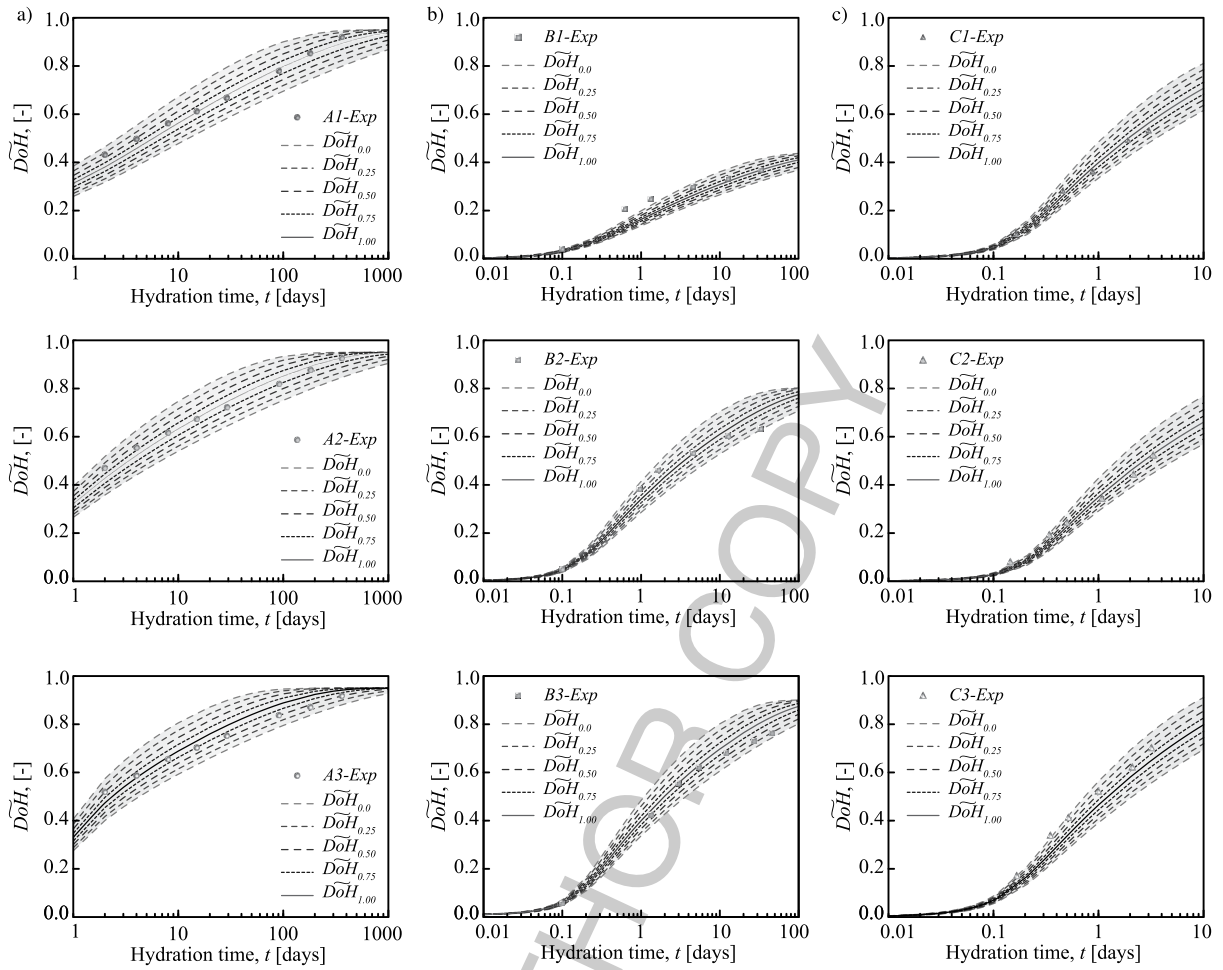


Fig. 6. Validation of fuzzy hydration curves: a) A1 to A3, b) B1 to B3, and c) C1 to C3.

to encompass the experimental values in the interval $[DoH_{0,0}^L, DoH_{0,0}^R]$. Notice, however, that B1 corresponds to an extreme case of w/c ; therefore, the imprecise prediction is related to a limitation of the affinity hydration model rather than the vagueness when estimating parameters.

The affinity model performs well on cements with different mineral composition in series C. Except for C2 and C3 at $t = 0.15$ and 0.35 days, respectively, the experimental data lies within $[DoH_{0,0}^L, DoH_{0,0}^R]$. A closer look at Fig. 6(c) indicates that, similarly to series A, the degree of fuzziness of the input parameters could be reduced for C1. Nevertheless, the same is not verified for C2 and C3, indicating that the variability in the compound composition of C2 and C3 is likely greater than in C1.

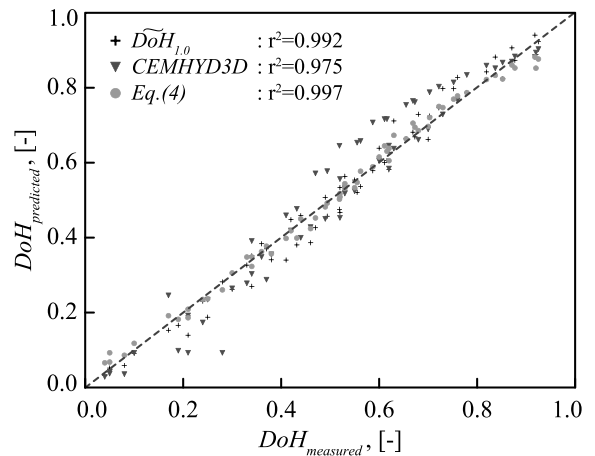


Fig. 7. Scatter plot of measured versus predicted DoH .

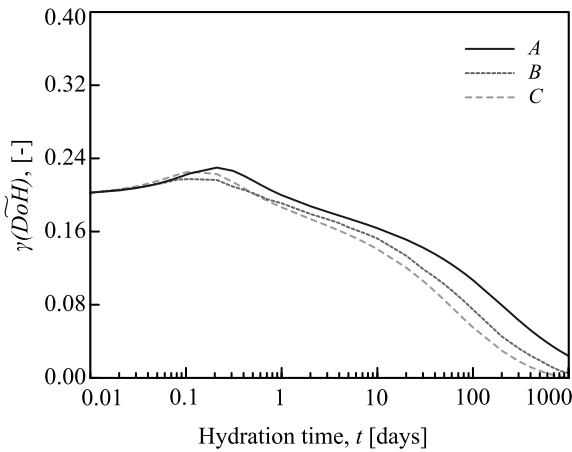


Fig. 8. Average degree of fuzziness in A, B, and C series.

The average $\gamma(\widetilde{DoH})$ obtained in each of the investigated series is illustrated in Fig. 8. It is evident that $\gamma(\widetilde{DoH})$ tends to decrease with hydration time. Such trend stems from the formulation of the affinity hydration model since it converges to DoH_∞ . In other words, as hydration proceeds to a known ultimate degree of hydration, the uncertainty in DoH estimation decreases.

Altogether, the results from Fig. 6 validate not only the fuzzy affinity hydration model for OPC hydration (Equation (18)) at various boundary conditions, but also Equations (13)–(17) for an estimation of the input parameters β_1 , β_2 , η , and DoH_∞ . Notice, however, that complementary investigations are likely necessary to verify whether the presented equations are robust enough to predict reliably the parameters of the fuzzy affinity hydration model for boundary conditions that differ from the ones explored in this paper.

6. Conclusions

Fuzzy set theory was used to address uncertainties when estimating affinity hydration model's parameters. Moreover, the extension principle was applied to derive the equations of the fuzzy affinity hydration model and compute the fuzzy solution in a simplified way. Different scenarios of hydrating Portland cement were simulated and the fuzzy model was verified against other models validated against experimental data.

The microstructure-property link presented in this paper, see Equations (13)–(15), provides β_1 , β_2 , η parameters directly from mineral composition and

Blaine fineness. The degree of fuzziness up to 20% extends their ranges, obtaining vague but reliable solutions regarding the degree of hydration. The fuzzy affinity hydration model proved suitable for predicting the degree of hydration of Ordinary Portland cement pastes with water-cement ratios ranging from 0.16 to 0.50, curing temperature ranging from 10 to 30°C, and various mineral compositions and *Blaine* fineness.

The verification results highlight the advantages of the fuzzy model with regard to its microstructure-property link and its performance when applied in complex tasks such as multiscale simulations. Hence, the fuzzy affinity hydration model represents a highly attractive prediction method for the cement and concrete industry since it includes only few parameters that are linked to cement properties and allows for tackling uncertainties in the parameter estimates while obtaining realistic results.

Future research prospects include the validation of the fuzzy affinity hydration model and the equations to estimate its input parameters on blended cements, e.g. slag and fly-ash cements, due to their high share in the market.

Acknowledgments

We gratefully acknowledge the support from the project “Support for improving teams in research and development and the development of intersectoral mobility at Czech Technical University in Prague” OP VK CZ.1.07/2.3.00/30.0034, which allowed for funding of Dr. da Silva's postdoctoral research. Also, the support from Competence Centres of the Technology Agency of the Czech Republic (TACR) under the project “Centre for Effective and Sustainable Transport Infrastructure” TE01020168 is acknowledged.

References

- [1] P.-C. Aitcin, Cements of yesterday and today: Concrete of tomorrow, *Cement and Concrete Research* **30**(9) (2000), 1349–1359.
- [2] American Society for Testing and Materials, *ASTM C150/C150M-12: Standard Specification for Portland Cement*, 2007.
- [3] D. Bentz, *A three-dimensional cement hydration and microstructure development modeling package*, Technical Report Version 3.0, NIST Building and Fire Research Laboratory, Gaithersburg, MD, 2000.
- [4] N. Branislavljevic and M. Ivetic, Fuzzy approach in the uncertainty analysis of the water distribution network of Becej, *Civil Engineering and Environmental Systems* **23**(3) (2006), 221–236.

- [5] J. Buckley and T. Feuring, Fuzzy differential equations, *Fuzzy Sets and Systems* **110**(1) (2000), 43–54.
- [6] M. Cervera, J. Oliver and T. Prato, Thermo-chemo-mechanical model for concrete. I: Hydration and aging, *Journal of Engineering Mechanics ASCE* **125**(9) (1999), 1018–1027.
- [7] C.-H. Cheng, A new approach for ranking fuzzy numbers by distance method, *Fuzzy Sets and Systems* **95**(3) (1998), 307–317.
- [8] T.-C. Chu, Ranking fuzzy numbers with an area between the centroid point and original point, *Computers & Mathematics with Applications* **43**(1–2) (2002), 111–117.
- [9] O. Coussy, *Mechanics of Porous Media*, Wiley, New York, 1995.
- [10] W.R.L. da Silva, V. Šmilauer and P. Štemberk, Analysis of the thermal behavior of mass concrete based on semi-adiabatic temperature measurements, In *Proceedings of Engineering Mechanics* (2013), pp. 518–527, Prague, Czech Republic, 2013.
- [11] W.R.L. da Silva, V. Šmilauer and P. Štemberk, Upscaling semi-adiabatic measurements for simulating temperature evolution of mass concrete structures, *Materials and Structures*, In press, 2013. doi: 10.1617/s11527-013-0213-3
- [12] W.R.L. da Silva and P. Štemberk, Expert system applied for classifying self-compacting concrete surface finish, *Advances in Engineering Software* **64** (2013), 47–61.
- [13] W.R.L. da Silva and P. Štemberk, Shooting-inspired fuzzy logic expert system for Ready-mixed concrete plants, *Journal of Intelligent and Fuzzy Systems* **25**(2) (2013), 481–491.
- [14] W.R.L. da Silva and V. Šmilauer, CEMHapp: Cement Hydration Application with GUI. Czech Technical University in Prague. Available at <http://concrete.fsv.cvut.cz/wilson/Software.html>.
- [15] J.I. Escalante-García, Nonevaporable water from neat opc and replacement materials in composite cements hydrated at different temperatures, *Cement and Concrete Research* **33**(11) (2003), 1883–1888.
- [16] J.I. Escalante-García and J.H. Sharp, Effect of temperature on the hydration of the main clinker phases in portland cements: Part I, neat cements, *Cement and Concrete Research* **28**(9) (1998), 1245–1257.
- [17] European Committee for, Standardization, *EN 197-1: Cement-Part 1: Composition, specifications and conformity criteria for common cements*, Brussels, 2000.
- [18] R. Fullér, On stability in possibilistic linear equality systems with lipschitzian fuzzy numbers, *Fuzzy Sets and Systems* **34**(3) (1990), 347–353.
- [19] D. Gawin, F. Pesavento and B.A. Schrefler, Hygro-thermochemo-mechanical modelling of concrete at early ages and beyond. Part I: hydration and hygro-thermal phenomena, *International Journal for Numerical Methods in Engineering* **67**(3) (2006), 299–331.
- [20] T.C. Hansen, Physical structure of hardened cement paste, A classical approach, *Matériaux et Constructions* **114**(19) (1986), 423–436.
- [21] L. Jendele, V. Šmilauer and J. Červenka, Multiscale hydro-thermo-mechanical model for early-age and mature concrete structures, *Advances in Engineering Software* **72** (2014), 134–146.
- [22] A. Kaufmann, *Introduction to the Theory of Fuzzy Subsets: Fundamental Theoretical Elements*, Vol. 1. Academic Press, New York, U.S. 1975.
- [23] P.S. Kechagias and B.K. Papadopoulos, Computational method to evaluate fuzzy arithmetic operations, *Applied Mathematics and Computation* **185**(1) (2007), 169–177.
- [24] G. Klir and B. Yuan, *Fuzzy sets and fuzzy logic: Theory and applications*, Prentice Hall, 1st edition, 1995.
- [25] K. Lee, editor, *First course on fuzzy theory and applications, Vol. 27 of Advances in Intelligent and Soft Computing*, Springer, 1st edition, 2004.
- [26] W. Lerch and C.L. Ford, Long-term study of cement performance in concrete: Ch. 3, *ACI Journal* **19**(8) (1948), 745–795.
- [27] F. Lin and C. Meyer, Hydration kinetics modeling of Portland cement considering the effects of curing temperature and applied pressure, *Cement and Concrete Research* **39**(2009) (2005), 255–265.
- [28] H.-T. Liu, An integrated fuzzy decision approach for product design and evaluation, *Journal of Intelligent and Fuzzy Systems* **25**(3) (2013), 709–721.
- [29] T. Matschei and F.P. Glasser, Temperature dependence, 0 to 40°C, of the mineralogy of Portland cement paste in the presence of calcium carbonate, *Cement and Concrete Research* **40**(5) (2010), 763–777.
- [30] J.-M. Mechling, A. Lecomte and C. Diliberto, Relation between cement composition and compressive strength of pure pastes, *Cement and Concrete Composites* **31**(4) (2009), 255–262.
- [31] R.H. Mills, Factors influencing cessation of hydration in water cured cement pastes. In *Proceedings of the Symposium on the Structure of Portland Cement Paste and Concrete*, Special Report No. 90, pp. 406–424, Highway Research Board, Washington D.C., 1966. Springer.
- [32] I. Pane and W. Hansen, Concrete hydration and mechanical properties under nonisothermal conditions, *ACI Materials Journal* **99**(6) (2002), 534–422.
- [33] X. Pang, D.P. Bentz, C. Meyer, G.P. Funkhouser and R. Darbe, A comparison study of portland cement hydration kinetics as measured by chemical shrinkage and isothermal calorimetry, *Cement and Concrete Research* **39** (2013), 23–32.
- [34] J.H. Park, J.S. Park, and Y.C. Kwun *Controllability for the semilinear fuzzy integrodifferential equations with nonlocal conditions*. In L. Wang, L. Jiao, G. Shi, X. Li, and J. Liu, editors, *Fuzzy Systems and Knowledge Discovery, Vol. 4223 of Lecture Notes in Computer Science*, pp. 221–230. Springer, Berlin Heidelberg, 2006.
- [35] L.J. Parrott, M. Geiker, W.A. Gutteridge and D. Killoh, Monitoring portland cement hydration: Comparison of methods, *Cement and Concrete Research* **20**(6) (1990), 919–926.
- [36] R. Revelli and L. Ridolfi, Fuzzy approach for analysis of pipe networks, *Journal of Hydraulic Engineering* **128**(1) (2002), 93–101.
- [37] A.K. Schindler and K.J. Folliard, Heat hydration models for cementitious materials, *ACI Materials Journal* **102**(1) (2005), 24–33.
- [38] J.H. Taplin, A method for following hydration reaction in portland cement paste, *Australian Journal of Applied Sciences* **10** (1969), 329–345.
- [39] V. Šmilauer and J. Krejčí, Multiscale model for temperature distribution in hydrating concrete, *International Journal for Multiscale Computational Engineering* **7**(2) (2009), 135–151.
- [40] V. Šmilauer, CemPy: A program for cement hydration with GUI. Czech Technical University in Prague. Available at <http://mech.fsv.cvut.cz/smilauer/index.php?id=software>
- [41] X.-Y. Wang, H.-S. and Lee, Modeling the hydration of concrete incorporating fly ash and slag, *Cement and Concrete Research* **40** (2010), 984–996.
- [42] P.P. Wang, D. Ruan and E.E. Kerre, editors, *Fuzzy Logic: A spectrum of theoretical & Practical issues, Vol. 215 of Studies in Fuzziness and Soft Computing*, Springer, 2007.
- [43] Y.-M. Wang, J.-B. Yanga, D.-L. Xua and K.-S. Chinc, On the centroids of fuzzy numbers, *Fuzzy Sets and Systems* **157**(7) (2006), 919–926.

- [44] Z.-X. Wang, J. Li and S. lin Gao, The method for ranking fuzzy numbers based on the centroid index and the fuzziness degree. In B. Cao, T.-F. Li and C.-Y. Zhang, editors, *Fuzzy Information and Engineering Volume 2, Vol. 62 of Advances in Intelligent and Soft Computing*, pp. 1335–1342. Springer, Berlin Heidelberg, 2009.
- [45] I. Wegener, *Complexity Theory: Exploring the Limits of Efficient Algorithms*, Vol. 1, Springer Berlin Heidelberg, Germany, 2005.
- [46] L.A. Zadeh, Fuzzy sets, *Information and Control* **8**(8) (1965), 338–353.
- [47] Q. Zhang, Y. Xiao and G.Wang, A new method for measuring fuzziness of vague set (or intuitionistic fuzzy set), *Journal of Intelligent and Fuzzy Systems* **25**(2) (2012), 505–515.

AUTHOR COPY